

Fluid Inclusions in VC-2B

Fluid inclusions were studied in fluorite from depths of 1273 and 1507 ft. and in calcite from 4293 ft. All of the inclusions studied were liquid-rich at room temperature. Vapor-rich inclusions were observed in the sample from 4293 ft. The presence of these inclusions, and the variable ice-melting temperatures of inclusions in this sample suggest that boiling may have occurred. No solid phases were observed in any of the inclusions. Only secondary inclusions were observed in the samples of fluorite. The inclusions in calcite form small isolated three dimensional arrays suggesting that they are primary.

Homogenization temperatures range from 144° to 274°C. No temperatures were obtained on the vapor-rich inclusions. The ice-melting temperatures of these inclusions range from -0.0° to -1.7°. Two distinct generations of inclusions with distinctly different homogenization temperatures and salinities are present in the fluorite from 1507 ft. One generation is characterized by homogenization temperatures that range from 144° to 149°C; the second by temperatures that range from 180° to 191°C. This latter group has similar homogenization temperatures but slightly higher apparent salinities than inclusions found at 1273 feet. No freezing measurements could be made on the lower temperature inclusions from 1507 ft. In every case, the bubble froze out during cooling and failed to renucleate before complete melting of the ice had occurred. The low temperature behavior of these inclusions suggest that their salinities are extremely low.

Inclusions from a depth of 4393 ft. display variable ice-melting temperatures ranging from -1.0° to -1.7°C. The generally similar homogenization temperatures (refer to T_m vs T_h plot) suggest that the differences in ice-melting temperatures results from variations in the CO_2 content of the fluids rather than from variations in the NaCl content of the fluids. This difference in the ice-melting temperatures (0.7°C) corresponds to a CO_2 of 1.6 wt. percent. The presence of the vapor-rich inclusions in this sample suggest that CO_2 was lost during boiling. Thus the actual salinity of these fluids may be closer to 1.7 wt. percent (computed in terms of NaCl).

Variations in the apparent salinities of the shallow fluids are also evident in the T_m vs T_h plot. This data suggests that the salinity of the shallow fluids is very low and that the fluids are enriched in CO_2 . Variations in the CO_2 of these fluids may also reflect gas loss due to boiling. The temperatures and salinities of these fluids suggest that they are steam-heated groundwaters.

11 5 2106
 11
 180
 186

WELL VC-2B		VALLES GEOTHERMAL AREA		prim. (p)				
Depth (ft)	(Th)L	Tm	NaCl wt%	Density (g/cc)	or sec. (s)	mineral	comments	
1273	178				s	Fluorite	along healed fracture	
1273	179	0.0	0.0	0.89	s	Fluorite	along healed fracture	
1273	179	-0.1	0.2	0.89	s	Fluorite	along healed fracture	
1273	193	0.0	0.0	0.88	s	Fluorite	along healed fracture	
1273	194	-0.2	0.4	0.88	s	Fluorite	along healed fracture	
1273	194	0.0	0.0	0.87	s	Fluorite	along healed fracture	
1273	194	-0.2	0.4	0.88	s	Fluorite	along healed fracture	
1273	195	-0.1	0.2	0.87	s	Fluorite	along healed fracture	
1273	195	0.0	0.0	0.87	s	Fluorite	along healed fracture	
1273	200	-0.4	0.7	0.87	s	Fluorite	along healed fracture	
1273	205	0.0	0.0	0.86	s	Fluorite	along healed fracture	
1507	2106	-0.4	0.7		s	Fluorite	along healed fracture	
1507	144				s	Fluorite	along healed fracture; bubble froze-out on freezing	
1507	144				s	Fluorite	along healed fracture; bubble froze-out on freezing	
1507	144				s	Fluorite	along healed fracture; bubble froze-out on freezing	
1507	145				s	Fluorite	along healed fracture; bubble froze-out on freezing	
1507	146				s	Fluorite	along healed fracture; bubble froze-out on freezing	
1507	146				s	Fluorite	along healed fracture; bubble froze-out on freezing	
1507	147				s	Fluorite	along healed fracture; bubble froze-out on freezing	
1507	147				s	Fluorite	along healed fracture; bubble froze-out on freezing	
1507	148				s	Fluorite	along healed fracture; bubble froze-out on freezing	
1507	149				s	Fluorite	along healed fracture; bubble froze-out on freezing	
1507	149				s	Fluorite	along healed fracture; bubble froze-out on freezing	
1507	180	-0.4	0.7	0.90	s	Fluorite	along healed fracture	
1507	181	-0.4	0.7	0.89	s	Fluorite	along healed fracture	
1507	182	-0.3	0.5	0.89	s	Fluorite	along healed fracture	
1507	183	-0.4	0.7	0.89	s	Fluorite	along healed fracture	
1507	183	-0.4	0.7	0.89	s	Fluorite	along healed fracture	
1507	184	-0.4	0.7	0.89	s	Fluorite	along healed fracture	
1507	184	-0.4	0.7	0.89	s	Fluorite	along healed fracture	
1507	186	-0.4	0.7	0.89	s	Fluorite	along healed fracture	
1507	186	-0.4	0.7	0.89	s	Fluorite	along healed fracture	
1507	186	-0.4	0.7	0.89	s	Fluorite	along healed fracture	
1507	191	-0.4	0.7	0.88	s	Fluorite	along healed fracture	
4393	2126	-1.5	2.6		p	Calcite	isolated three-dimensional array	
4393	256	-1.7	2.9	0.81	p	Calcite	isolated three-dimensional array	
4393	259	-1.0	1.7	0.80	p	Calcite	isolated three-dimensional array	
4393	273				p	Calcite	isolated three-dimensional array	
4393	273	-1.5	2.6	0.78	p	Calcite	isolated three-dimensional array	
4393	274	-1.7	2.9	0.78	p	Calcite	isolated three-dimensional array	
4393	274	-1.7	2.9	0.78	p	Calcite	isolated three-dimensional array	
4393	275	-1.5	2.6	0.78	p	Calcite	isolated three-dimensional array	
4393	277	-1.5	2.6	0.77	p	Calcite	isolated three-dimensional array	

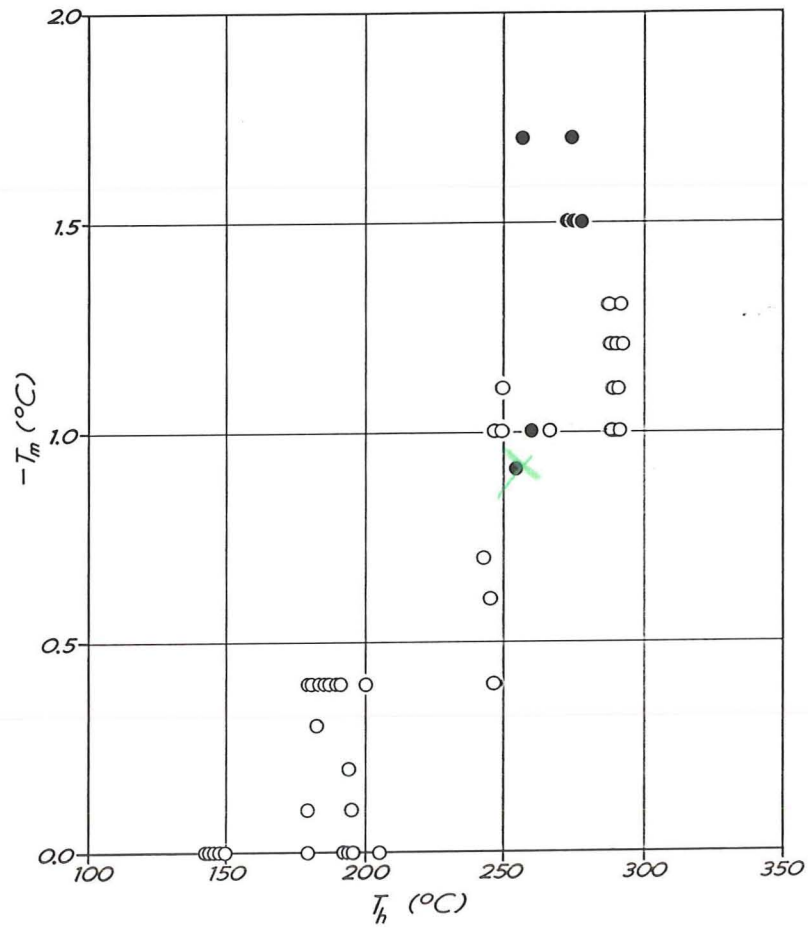
146
 11 5 169
 11
 180
 186

2161
 270
 8 5 2161
 16
 180
 186

184
 11 5 2126
 11
 180
 186

UC2B RD011 TEMPERA

DATE	DEPTH	TEMP. F	TEMP. C
8/7	715	180	82
8/7	720	170	77
8/7	743	180	82
8/7	768	200	93
8/8	778	230	110
8/8	818	170	77
8/9	870	160	71
8/15	1433	180	82
8/17	1575	220	104
8/17	1608	230	110
8/17	1633	230	110
8/18	1648	235	113
8/18	1653	190	88
8/18	1678	190	88
8/18	1698	230	110
8/19	1713	230	110
8/19	1723	225	107
8/19	1728	230	110
8/19	1733	230	110
8/19	1738	225	107
8/19	1743	230	110
8/19	1763	240	116
8/20	1797	220	104
8/20	1802	230	110
8/20	1823	240	116
8/21	1828	250	121
8/21	1833	250	121
8/21	1838	230	110
8/21	1863	230	110
8/21	1868	260	127
8/21	1878	290	143
8/21	1898	290	143
8/21	1908	300	149
8/21	1918	290	143
8/21	1948	290	143
8/22	1981	300	149
	1988	290	143
	1996	300	149
8/22	2003	290	143
8/23	2023	330	166
	2028	300	149
	2033	290	143
	2038	340	171
	2043	320	160
	2073	320	160
8/23	2078	340	171
9/2	2094	380	193
9/3	2143	390	199
	2163	400	204
	2183	420	216



	$T_i, ^\circ\text{C}$	SiO_2	Na	K	Ca	Mg	Li	HCO_3	SO_4	Cl	B	As	T_e	
VC-2A	210	322	1888	309	5.5	0.43	18.8	57	56	2745	10.2	1.81	-0.32	(one entry) 490 m
B-15	267	441	1196	261	12.4	0.02	15	48	29	2093	17	2.3	-0.21	produced: composite wellhead
B-13	278	546	1146	244	3.4	0.04	17	168	42	1897	17	1.6	-0.20	"
WC23-4	214	395	2800	470	80.5	2.89	28.2	360	33	4350	37.3	NA	-0.47	(one entry) 1463 m
WC23-4	233	450	5890		46.0	0.45	68	382	95	9960	96.2	NA	-0.92	(one entry) 1920 m

Calculations used $T_{\text{NaK}} + T_{\text{SiO}_2} = T_e$ (column 2, above)

- Remember, the real ones may have gas, which is not in the T_m derived above.

Geothermometers

$T_m @ \text{Geoth Temp} = T_h$

Sample	Na/K	Na/K/Cl	Qtz	Na/K	Na/K/Cl	Qtz	Neas
VC-2A	263 ^(loss Ca)	281	252	-0.32	-0.32	-0.32	-0.32
B-15	294	281	247	-0.21	-0.21	-0.21	-0.21
B-13	292	295	250	-0.20	-0.20	-0.20	-0.20
WC23-4	266	258	249	-0.47	-0.47	-0.47	-0.47
WC23-4			248	-	-	-	-0.92

	T, °C	SiO ₂	Na	K	Ca	Mg	Li	HCO ₃	SO ₄	Cl	B	As	T _g	
VC-2A (252)	210	322	1888	309	5.5	0.43	18.8	57	56	2945	18.2	1.81	-0.32	(one entry) 490 m
B-15 (247)	267	441	1196	261	12.4	0.02	15	48	29	2093	17	2.3	-0.21	productive composite well head
B-13 (250)	278	546	1146	244	3.4	0.04	17	168	42	1897	17	1.6	-0.20	(")
WC23-A (249)	214	395	2800	470	80.5	2.89	28.2	360	33	4350	39.3	NA	-0.47	(one entry) 1463 m
WC23-A (240)	233	450	5890	1020	46.0	0.45	68	382	95	9960	96.2	NA	-0.92	(one entry) 1920 m

Q NukB
243. n280

Calculations used $T_{NaK} + T_{SiO_2} = T_g$ (column 12, above)

- Remember, the real ones may have gas, which is not in the T_m derived above.

e/flinc

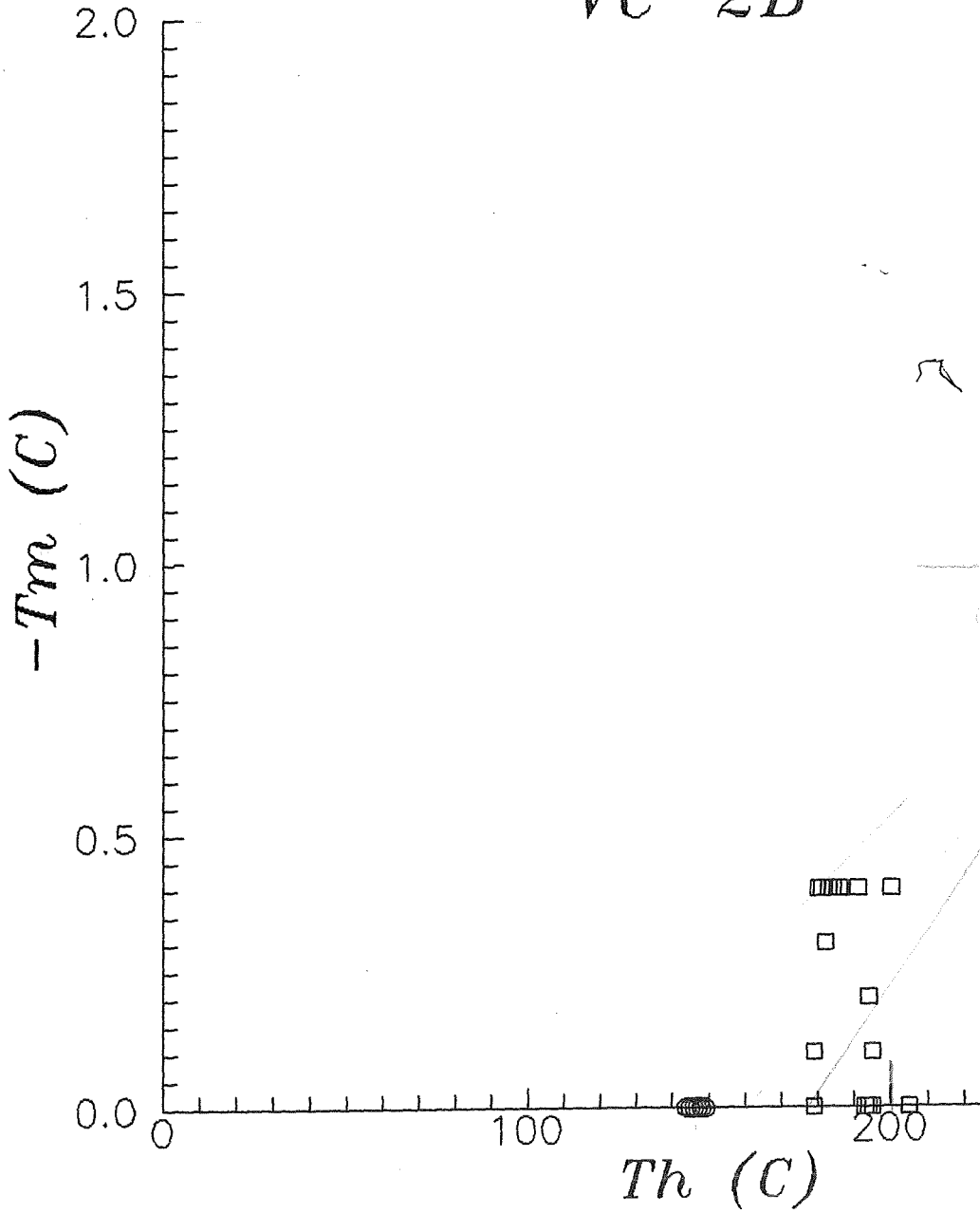
calculated using FLINC prog^o
written by M. Adams

Henry's Law

uses R's La wellhead
Henry's eq of Potter wellhead
from

known T
measured composition and
known T

VC-2B



Sample	Qtz	QtzAd	Na/K(F)	Na/K(G)	NaKCa	KMg	(f)
VC-2A 210	215	196	263	275	281	236	17
B-15 262	241	217	294	303	281	317	5
B-13 265	204	187	292	301	295	290	17
WC23-4 214	232	210	266	277	258	211	5
WC23-4 233	243	218	269	280	287	304	23

A reconnaissance study of fluid inclusions in vein quartz, fluorite, and calcite was conducted to better characterize temperature and compositional relationships within the reservoir. Samples were collected from depths ranging from 1273 to 5751. All of the inclusions studied were liquid-rich, and contained two phases at room temperature. The inclusions in fluorite and quartz were secondary in origin, occurring along healed fractures. Primary liquid and vapor-rich inclusions which define isolated three dimensional arrays were observed in coarse-plates of calcite (fish-scales). Because of the small size of the vapor-rich inclusions (less than microns), it was not possible to make reliable microthermometric measurements on them. Their presence, however, and the morphology of the calcite crystals suggests that mineral deposition occurred as a result of boiling.

The results of the microthermometric measurements are shown in Figure . The homogenization temperatures of the inclusions ranged from 144 to 274°C. With the exception of fluorite from a depth of 1507 feet, individual crystals displayed little variation in homogenization temperatures. In contrast, two distinct generations of secondary inclusions were observed in the fluorite. One generation is characterized by homogenization temperatures that ranged from 180 to 191°C, the second by temperatures between 144 and 149°C. No freezing measurements were conducted on the group of lower temperature inclusions because in every case, the bubble froze out and failed to renucleate before complete melting had occurred. Thus, while it was not possible to compare the composition of the two sets of inclusions, the temperature behavior of these inclusions indicates that they had low salinities.

Ice-melting temperatures of the inclusions ranged from 0.0 to -1.7. Despite their narrow range of homogenization temperatures, several of the samples displayed large variations in their freezing point depressions. For example, the ice-melting temperatures of inclusions in calcite from 4393 feet ranged from -1.0 to -1.7°C while the homogenization temperatures varied by only 21°C.

The large range in ice-melting temperatures cannot be readily explained solely in terms of variations in the salinities of the inclusion fluids since this would imply salinities that ranged from 1.7 to 2.9 equivalent weight percent NaCl during formation of the calcite (Potter et al., 1978). Alternatively the variations in ice-melting temperatures may be due largely to variations in the gas contents of the fluids (Hedenquist and Henley, 1985). For this sample, the differences in ice-melting temperatures of the inclusions (0.7°C) corresponds to a CO₂ content of 1.9 weight percent. Large variations in CO₂ may be caused by gas loss or gas enrichment related to boiling. Where such variations in ice-melting temperatures exist, an estimate of the salinity of the fluid can be obtained from the minimum freezing point depression. Thus, the salinity of the fluids trapped at a depth of 4393 is probably close to 1.7 equivalent weight percent NaCl. This value is consistent with the fluids sampled from a similar depth in WC2B-4 which have a calculated

ice-melting temperature (gas-free) of -0.92 and a quartz geothermometer temperature of 248°C .

The relationships between the homogenization and ice-melting temperatures suggest that the inclusion fluids in different samples can be related to each other by dilution. The high temperature endmember was sampled at a depth of 5751 feet. The fluid has a temperature of 290°C , a salinity of 1.7 equivalent weight percent NaCl, and a CO_2 content of 0.84 weight percent. The low temperature endmember was trapped in fluorite in the upper part of the well. This fluid has a temperature of about 190°C , a low salinity, and a variable gas content. These relationships suggest that the fluid represents a steam-heated groundwater. A lowering of the water table may be responsible for the formation of lower temperature inclusions in the fluorite (Sasada, 1988)

References

Hedenquist, J. W., and Henley, R. W., 1985, The importance of CO_2 on freezing point measurements of fluid inclusions: Evidence from active geothermal systems and implications for epithermal ore deposition: *Econ. Geol.*, v. 80, p. 1379-1406.

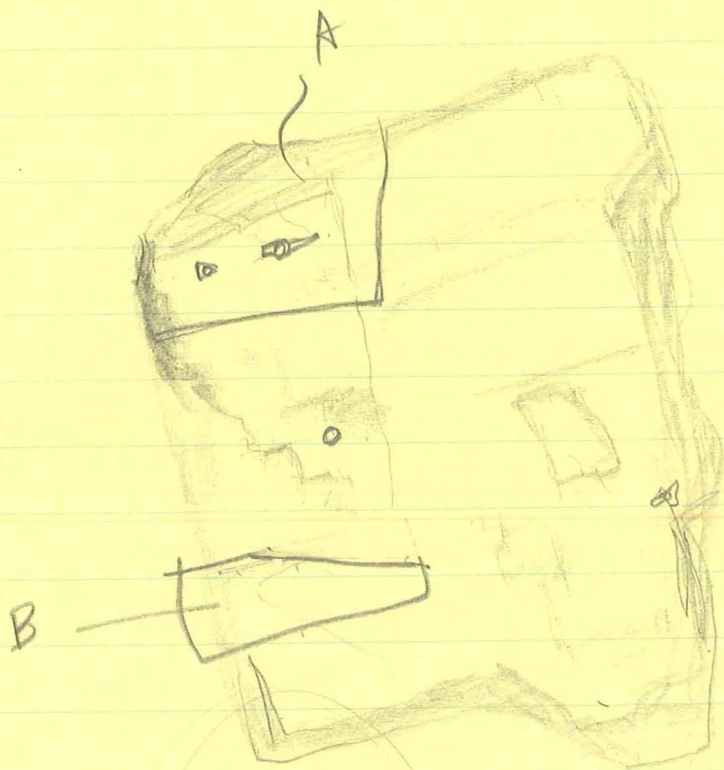
Potter, R. W., II, Clynne, M. A., and Brown, D. L., 1978, Freezing point depression of aqueous sodium chloride solutions: *Econ. Geol.*, v. 73, p. 284-5.

Sasada, M., 1988, Microthermometry of fluid inclusions from VC-1 core hole in Valles Caldera, New Mexico: *Jour. Geophys. Res.*, v. 90, p. 6091-6096

BACA					prim. (p)	
Depth(ft)	Th	Tn	NaCl wt%	Density (g/cc)	or sec. (s)	mineral
3283	249	-1.0	1.7	0.81	s	Cc
3283	254	-0.9	1.6	0.80	p?	Cc
3283	267	-1.0	1.7	0.78	s	Cc
3283	249	-1.0	1.7	0.81	p?	Cc
3283	261				p?	Cc
3283	245	-0.1	0.2	0.80	s	Cc
3283	244	-0.6	1.0	0.81	s	Cc
3283	242	-0.7	1.2	0.82	s	Cc
3283	246	-0.4	0.7	0.81	s	Cc
3283	245				s	Cc
3283	246	-1.1	1.9	0.82	?	Cc
3283	237				s	Cc
5751	291	-1.2	2.1	0.74	s	Qtz
5751	291	-1.0	1.7	0.74	s	Qtz
5751	291	-1.1	1.9	0.74	s	Qtz
5751	289	-1.1	1.9	0.74	s	Qtz
5751	289	-1.0	1.7	0.74	s	Qtz
5751	290	-1.2	2.1	0.75	s	Qtz
5751	288	-1.3	2.2	0.75	s	Qtz
5751	288				s	Qtz
5751	289	-1.0	1.7	0.74	s	Qtz
5751	289	-1.0	1.7	0.74	s	Qtz
5751	291	-1.2	2.1	0.74	s	Qtz
5751	291	-1.2	2.1	0.74	s	Qtz
5751	291	-1.3	2.2	0.75	s	Qtz
5751	291	-1.3	2.2	0.75	s	Qtz
5751	292				s	Qtz

BACA
3283

big ones
do last
2 void stretchy



think in CO2

$$\bar{x} = 249.55 \pm 7.55$$

$$231.3 - 267.2$$

S (12) $\frac{246.2}{246.5}$ (-1.1)

S (11) 237.3°
too small to trace

S (1) $\frac{249.3}{247.4}$ (-1.0)

P? (2) $\frac{254.5}{254.2}$ (+3)

S (3) 267.2 (-1.0)

P? (4) $\frac{249.2}{249.1}$

P? (5) $\frac{261.2}{261.4}$ (-1.2)

S (6) $\frac{244.4}{244.4}$ (-1)

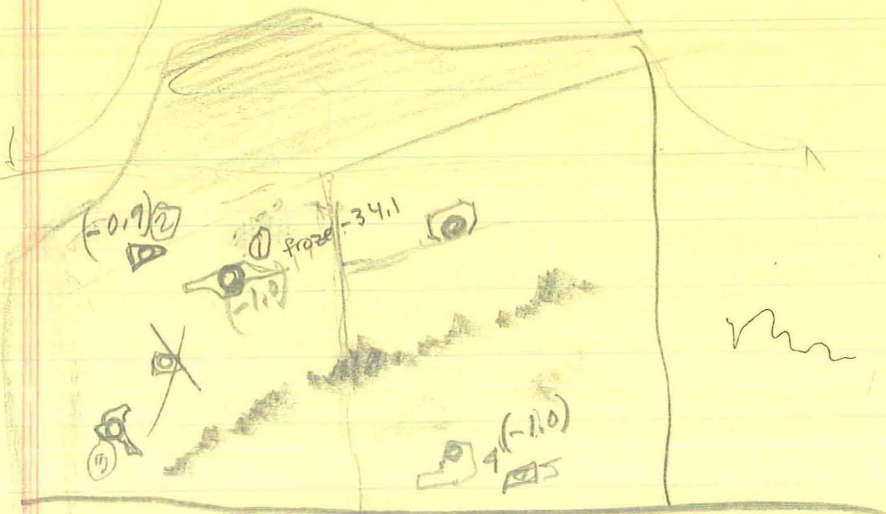
S (7) 244.3 (-6)

S (8) 242.3 (-7)

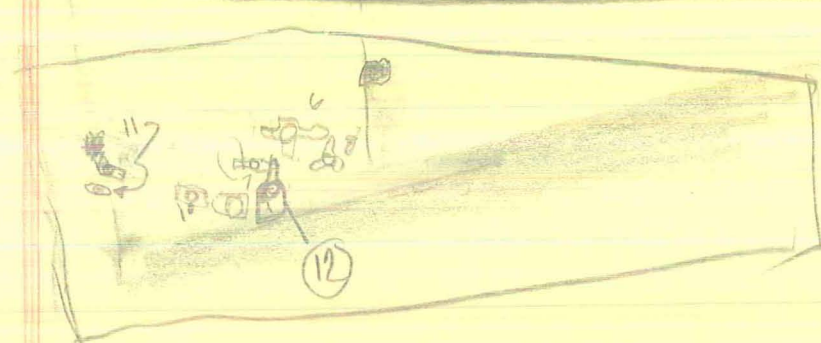
S (9) 245.6 (-4)

S (10) 244.9 too small

Hand



(A)

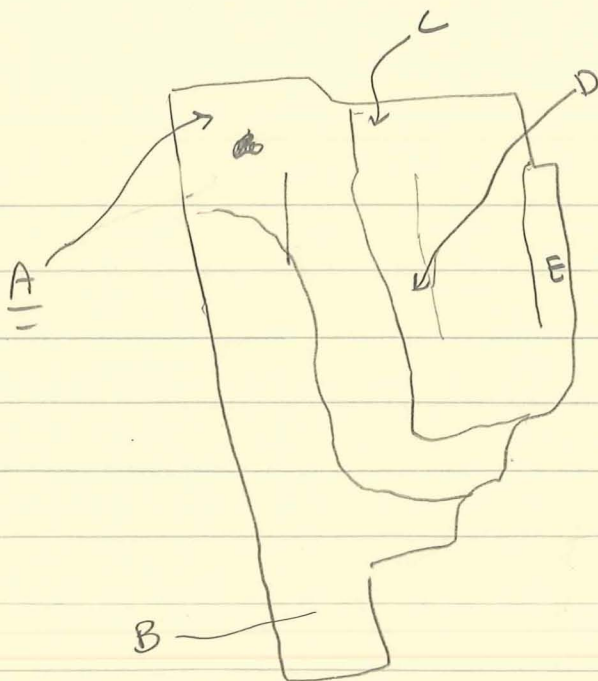


(B)

BACA 5751

1-31-89
2-1-89

all secondary



1. 291.0 s. planar
291.0 R (-1.2)

s. 2. >289.7 (-1.0)
>290.3
>290.7
<291.1
291.0

s. 3. >289.2
290.7
-1.1 290.6 R

4. 289.23
s. 289.2 R
-1.1

s. 5. 288.5
-1.0

s. 6. 289.5
-1.2

s. 7. 288.0
-1.3

s. 8. 288.0
Too small

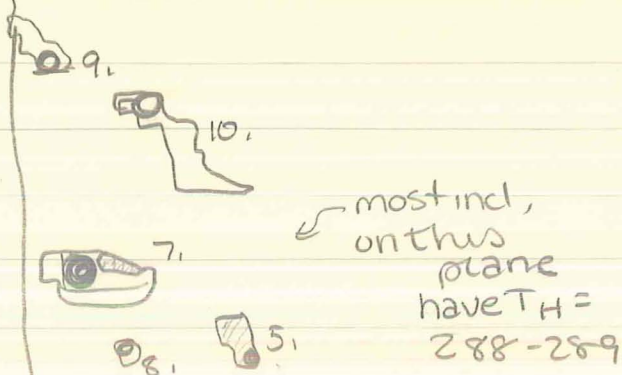
s. 9. 289.1
-1.0 289.1 R

s. 10. 289.1
-1.0 289.1 R

A

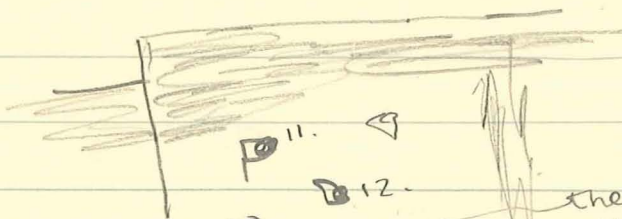


B



9.6

C



S. 11. > 288
 < 290.3
 (-1.2) (291.0)

these
 all have
 same TH
 ~290-
 291

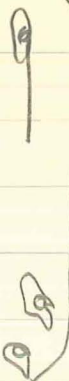
S. 12. > 285
 < 290.3
 (-1.2) < 291.1
 (291.0)
 291.0R

D



13. > 289.5
 < 291
 < -1.3 < 290.4
 (-1.3) (290.8)

14.



all on
 this plane
 went at
 290.5-
 291

14 > 290.4
 < -1.3
 (-1.3) (290.8)
 290.8R

E



S. 15. > 290.8 (291.7)
 < 291.7
 291.5 291.6R

Tm?